J. Appl. Comput. Mech., 4(4) (2018) 260-274
DOI: 10.22055/JACM.2017.23591.1164

ISSN: 2383-4536
jacm.scu.ac.ir

Shahid Chamran University of Ahvaz

Journal of Applied and Computational Mechanics

Research Article

Stability Analysis of a Strongly Displacement Time-Delayed Duffing Oscillator Using Multiple Scales Homotopy Perturbation Method

Yusry O. El-Dib

Department of Mathematics, Faculty of Education, Ain Shams University,

Roxy, Cairo, Egypt, yusryeldib52@hotmail.com

Received October 04 2017; Revised December 13 2017; Accepted for publication December 15 2017.
Corresponding author: Yusry O. El-Dib, yusryeldib52@hotmail.com

Abstract. In the present study, some perturbation methods are applied to Duffing equations having a displacement time-delayed variable to study the stability of such systems. Two approaches are considered to analyze Duffing oscillator having a strong delayed variable. The homotopy perturbation method is applied through the frequency analysis and nonlinear frequency is formulated as a function of all the problem's parameters. Based on the multiple scales homotopy perturbation method, a uniform second-order periodic solution having a damping part is formulated. Comparing these two approaches reveals the accuracy of using the second approach and further allows studying the stability behavior. Numerical simulations are carried out to validate the analytical finding.

Keywords: Homotopy perturbation method, Multiple scales method, Frequency analysis, Periodic nonlinear solution, Stability analysis, Displacement delay Duffing oscillator.

1. Introduction

This paper concerns with the effect of a displacement time-delayed Duffing type oscillator. The purpose is to find nontrivial solutions and investigate the stability analysis. The corresponding system consists of a strong nonlinear time-delayed Duffing oscillator which is governed by the following second-order nonlinear differential equation:

$$\frac{d^2y}{dt^2}+\mu\frac{dy}{dt}+\omega^2 y+Qy^3=\eta y\left(t-\tau\right),\quad y\left(0\right)=1;\ \dot{y}(0)=-1, \tag{1}$$

where μ,η,Q,τ, and ω are real physical quantities describing the damping, coefficient of delay, coefficient of nonlinearity, time delay, and the natural frequency, respectively. The Duffing equation is used to model the nonlinear dynamics of special types of electrical and mechanical systems. This differential equation, named after the studies of Duffing in 1918 [1], has a cubic nonlinearity and describes an oscillator. It has drawn extensive attention due to the richness of its chaotic behavior with a variety of interesting bifurcations. Some of its applications are in electronics, mechanics, electromechanics, and biology. On the other hand, the brain is full of oscillators at micro and macro levels [2]. In addition, it has many applications in neurology, ecology, secure communications, cryptography, and chaotic synchronization.

Equation (1) may serve as the simplest model for describing the dynamic of various controlled physical and engineering systems [3–5]. Other works have been devoted to study the dynamic of a Duffing oscillator under a delayed feedback control [6]. In addition, Eq. (1) has been considered in a study [7] as a simple model for a vibration problem in turning machine for

Published Online: Sep 20 2018

modelling the nonlinear generative effect in metal cutting [3] or for exploring the control of a flexible beam in a simple mode approach [8].

Nonlinear oscillation problems are important issues in engineering, physical science, applied mathematics, mechanical structures, nonlinear circuits, chemical oscillation, and many real world applications. Nonlinear vibrations of oscillation systems are modeled by nonlinear differential equations. In most of these cases, it is often more difficult to get exact solution of these nonlinear problems. To solve this problem, many researchers developed analytical approximate solutions using various analytical techniques. One of the most important methods of solving nonlinear differential equations is the homotopy perturbation method [9–19]. The homotopy perturbation is a technique that allows obtaining solutions without the restriction of small parameter. The homotopy perturbation method is a relatively new method [20-26] which is still evolving similar other methods and has theoretical and application limitations. The method was first introduced by He in late 1990s [9, 10]. The initial method has been developing very fast and it's the main progress was the homotopy perturbation method with two expanding parameters [14] and the homotopy perturbation method with an auxiliary term [15]. Homotopy perturbation method with two expanding parameters was studied by He [15]. The parameterized homotopy perturbation method was addressed by Adamu and Ogenyi [24] as a modification of the homotopy perturbation method. El-Dib [25 & 26] applied the modulate method to the homotopy perturbation which allows studying the stability behavior of strongly nonlinear oscillators. In a study [26], El-Dib suggests a modified version of the homotopy perturbation method by adopting the multiple scales method. This modification works especially well for nonlinear oscillators.

Delay differential equations are considered as an important tool for the modeling of dynamical phenomena in various fields of science including neuroscience, optoelectronics, and biological or mechanical systems. They allow for the description of potentially high dimensional dynamical effects caused by a delayed feedback or control, aging, and finite transmission speed. From a mathematical point of view, they represent an important class of dynamical systems and can be studied by advanced mathematical methods, including bifurcation theory, singular perturbations, or semi-group theory. Delayed differential equations are used to describe many physical phenomena of interest in biology, medicine, chemistry, physics, engineering, and economics. Kruthika et al. [27] analyzed the local stability of a gene-regulatory network and immunotherapy of cancer. They are modeled as nonlinear time-delayed systems.

In recent years, much interest has been devoted to the study of the dynamics of circuits described by nonlinear equations with delay, which exhibit chaotic attractors; interesting applications in secure communications [28] have been found. The study of the dynamic behavior of such circuits is very difficult.

Recently, many authors have studied the existence of periodic solutions of the Duffing as given in Eq. (1) by using various methods and techniques. The effect of a high-frequency excitation on nontrivial solutions and biostability in a delayed Duffing oscillator with a delayed displacement feedback was investigated by M. Hamdi and M. Belhaq [29]. Rafa Rusinek et al. [30] presented the analytical and numerical investigation of externally forced Duffing oscillator with delayed displacement feedback. The constrained optimization harmonic balance method was applied by Liao and Sun [31]. Their study dealt with the time-delayed Duffing oscillator and the analytical formulation of the nonlinear equality constraints was derived. Therefore, the gradients of the nonlinear equality were obtained. On the other hand, the improved constrained optimization harmonic balance method was presented by Liao [32]. He solved the Duffing oscillator with time delayed term. S. Sah and R. Rand [33] studied the dynamics of nonlinear systems that were subjected to delayed self-feedback. They considered two approaches to analyze the Hop bifurcations in such slow flows. In the first approach, they replaced the delayed variables in the slow flow with non-delayed variables. In the second approach, they kept the delayed variables in the slow flow. The goal of the present study is to investigate the role of the displacement time-delay parameter on the stability of a strong Duffing equation.

Over the past two decades, more effort has been invested in the analysis and synthesis of time-delayed uncertain systems. Various results have been obtained such as providing finite-dimensional sufficient conditions of stability. Away from the classical linear perturbation technique which depends on small parameter, El-Dib [34] applied the multiple scale method to study the stability behavior for three coupled Mathieu equations having displacement delayed variables.

Since the introduction of the first delayed models, many publications have appeared to summarize theorems and Homotopy method into a solution that deals with the properties of delayed systems [35–38]. Alomari and coworkers [37] developed an algorithm to obtain approximate analytical solutions of the delayed differential equations by using the homotopy analysis and the modified homotopy analysis methods. They used their method to obtain an approximate solution for various linear and nonlinear differential equations, while their numerical predictions agreed with the numerical integration solutions. Olvera et al. [38] applied the enhanced multistage homotopy perturbation method to solve delayed differential equations with constant and variable coefficients. This method was based on a sequence of subintervals that provided approximate solutions. This method cannot be applied to study the properties of stability.

The stability behavior of a Duffing equation having a displacement time-delayed variable is the aim of the present study. The perturbation methods for such systems give rise to flows which characteristically contains delayed variable. Two approaches are considered to analyze such strongly time-delayed Duffing oscillators.

2. Basic Idea of the Homotopy Perturbation Method

In the homotopy perturbation method [9-15], a general nonlinear equation is considered as follows:

$$L(y)+N(y)=f(t), \tag{2}$$

with initial condition: $y(0)=A$ and $\dot{y}(0)=B$, where L is an auxiliary linear operator, N is a nonlinear operator, and

$f(t)$ is the inhomogeneous part. The concept of homotopy is constructed in the following one-parameter family of equations:

$$H(y,\rho)=(1-\rho)\left[L(y)-L(u_0)\right]+\rho\left[L(y)+N(y)-f(t)\right]=0,\quad \rho\in[0,1] \tag{3}$$

$$H(y,\rho)=L(y)-L(u_0)+\rho\left[L(u_0)+N(y)-f(t)\right]=0,\quad \rho\in[0,1] \tag{4}$$

where ρ is the embedding parameter called a bookkeeping parameter and u_0 is the initial guess. The embedding parameter is monotonically increases from zero to unity. It is obvious that when $\rho\to 0$, Eq. (2) becomes a linear differential equation, $L(y)=0,$ for which an exact solution can be calculated. As $\rho\to 1,$ it becomes the original nonlinear one. Therefore, the changing process of ρ from zero to unity is just that of Eq. (2) to Eq. (1). According to the standard homotopy perturbation method [9–15], the solution may be expanded in a power series of ρ as follows:

$$y(t,\rho)=y_0(t)+\rho y_1(t)+\rho^2 y_2(t)+\rho^3 y_3(t)+\dots. \tag{5}$$

Often, one iteration method cannot be done due to the complicated nonlinear equation. Therefore, an additional iteration method is needed. In such cases, the perturbed natural frequency ω might be useful. Using the parameter ρ as an expanding parameter the following relation is obtained:

$$\Omega^2(\rho)=\omega^2+\rho\omega_1+\rho^2\omega_2+\dots \tag{6}$$

where ω is known as a linear frequency and ω_j are unknowns determined from the solvability conditions that are arising by removing the secularity. This secularity is produced, in each order of perturbation, due to the inhomogeneity in equations describing the various perturbation orders.

The complete solution of the nonlinear problem is obtained as $\rho\to 1,$ therefore, the following relation is obtained:

$$y(t)=\lim_{\rho\to 1} y(t,\rho)=y_0(t)+y_1(t)+y_2(t)+y_3(t)+\dots \tag{7}$$

Moreover, the frequency ω is obtained as $\rho\to 1$ at the final form. It is known as the approximate nonlinear frequency ω_N :

$$\omega_N^2=\lim_{\rho\to 1}\Omega^2(\rho)=\omega^2+\omega_1+\omega_2+\dots \tag{8}$$

To study the stability behavior, El-Dib's modification [26] for the homotopy perturbation method is needed to be applied. In this modification, the function $y(t)$, for $\rho>0$, is replaced by $Y(T_0,T_1,T_2,..T_n)$ with $T_n\equiv\rho^n t, n=0,1,2,3,...$ based on the previous studies [39, 40], the first and second derivatives might be replaced by the following expansions:

$$\frac{d}{dt}=\frac{\partial}{\partial T_0}+\rho\frac{\partial}{\partial T_1}+\rho^2\frac{\partial}{\partial T_2}\dots \tag{9}$$

$$\frac{d^2}{dt^2}=\left[\frac{\partial^2}{\partial T_0^2}+2\rho\frac{\partial^2}{\partial T_0\partial T_1}+\rho^2\left(\frac{\partial^2}{\partial T_1^2}+2\frac{\partial^2}{\partial T_0\partial T_2}\right)\dots\right]. \tag{10}$$

The function $y(t,\rho)$ may be expanded as

$$y(t,\rho)=Y_0(T_0,T_1,T_2,..)+\rho Y_1(T_0,T_1,T_2,..)+\rho^2 Y_2(T_0,T_1,T_2,..)+\dots \tag{11}$$

The above-mentioned relation represents one expansion and two perturbations; the first is the independent variable t and the other is the dependent variable $y(t)$ [39, 40]. One of the most important steps in the application of standard homotopy perturbation method is to construct a suitable homotopy equation, which can approximately describe the solution properties when homotopy parameter is zero. Therefore, the multiple-scales homotopy statement can be constructed with zero initial guess as follows:

$$H(y,\rho)=L\left[Y(T_0,T_1,T_2,..;\rho)\right]+\rho\left\{N\left[Y(T_0,T_1,T_2,..;\rho)\right]-f(T_0)\right\}=0,\quad \rho\in[0,1]. \tag{12}$$

The complete solution for the nonlinear problem is obtained as $\rho\to 1,$ therefore, the following relation is obtained:

$$y(t)=\lim_{\rho\to 1} Y(T_0,T_1,T_2,..;\rho)=y_0(t)+y_1(t)+y_2(t)+y_3(t)+\dots \tag{13}$$

Frequency Response Analysis Using Homotopy Perturbation Method of Eq. (1). This section is concerned with the first technique which is known as the frequency responses analysis. In this method, an expansion of the dependent variable $y(t)$

is taken into consideration. Moreover, the nonlinear frequency is perturbed around the linear frequency ω^2 [41, 42, & 43]. The application of the secularity conditions leads to determination of the unknown Eigen frequencies. Therefore, the uniform solutions should be obtained. The complete solution is formulated by setting the Homotopy parameter ρ to be a unity. This procedure is done as follows:
Defining the two parts $L(y)$ and $N(y)$ as

$$L(y) = \ddot{y} + \omega^2 y, \qquad N(y) = \mu \frac{dy}{dt} + Qy^3 - \eta y(t-\tau). \tag{14}$$

the homotopy can be built with zero initial guess as

$$H(y,\rho) = \ddot{y} + \omega^2 y + \rho\left(\mu \frac{dy}{dt} + Qy^3 - \eta y(t-\tau)\right) = 0; \quad \rho \in [0,1] \tag{15}$$

Expanding both the function $y(t,\rho)$ and the natural frequency ω^2 as defined by expansions (4) and (5) in addition to substituting (4) and (5) into (3) and setting them to zero like powers of ρ, the following relations are obtained:

$$\rho^0 : \ddot{y}_0 + \Omega^2 y_0 = 0; \; y_0(0) = 1, \; \dot{y}_0(0) = -1. \tag{16}$$

$$\rho^1 : \ddot{y}_1 + \Omega^2 y_1 = \omega_1 y_0 - \mu \dot{y}_0 - Qy_0^3 + \eta y_0(t-\tau); \; y_1(0) = 0, \; \dot{y}_1(0) = 0 \tag{17}$$

$$\rho^2 : \ddot{y}_2 + \Omega^2 y_2 = \omega_1 y_1 + \omega_2 y_0 - \mu \dot{y}_1 - 3Qy_0^2 y_1 + \eta y_1(t-\tau); \; y_2(0) = 0, \; \dot{y}_2(0) = 0 \tag{18}$$

Considering initial conditions, the solution of Eq. (16) yields

$$y_0(t) = \cos\Omega t - \frac{1}{\Omega}\sin\Omega t. \tag{19}$$

Accordingly,

$$y_0(t-\tau) = \cos\Omega(t-\tau) - \frac{1}{\Omega}\sin\Omega(t-\tau). \tag{20}$$

with the help of Eqs. (19) and (20), the first-order problem, Eq. (17), becomes

$$\begin{aligned} \ddot{y}_1 + \Omega^2 y_1 = &\left\{\omega_1 - \mu - \frac{3}{4}Q\left(1 + \frac{1}{\Omega^2}\right) + \eta\cos\Omega\tau + \eta\frac{1}{\Omega}\sin\Omega\tau\right\}\cos\Omega t \\ &- \frac{1}{\Omega}\left[\omega_1 + \mu\Omega^2 - \frac{3Q}{4}\left(1 + \frac{1}{\Omega^2}\right) - \eta\Omega\sin\Omega\tau + \eta\cos\Omega\tau\right]\sin\Omega t \\ &- \frac{Q}{4}\left(1 - \frac{3}{\Omega^2}\right)\cos 3\Omega t + \frac{Q}{4\Omega}\left(3 - \frac{1}{\Omega^2}\right)\sin 3\Omega t. \end{aligned} \tag{21}$$

The investigation of Eq. (21) reveals that there is a source of secular terms. The secular terms are corresponding to $(\cos\Omega t)$ and $(\sin\Omega t)$. The elimination of these secular terms yields

$$\omega_1 = \tfrac{1}{2}\left(1 - \Omega^2\right)\mu + \frac{3Q}{4}\left(1 + \frac{1}{\Omega^2}\right) + \tfrac{1}{2}\eta\left(\Omega - \frac{1}{\Omega}\right)\sin\Omega\tau - \eta\cos\Omega\tau \tag{22}$$

The solution of Eq. (21), away from secular terms, is given by

$$y_1(t) = -\frac{Q}{32\Omega^2}\left(1 - \frac{3}{\Omega^2}\right)\left(\cos\Omega t - \cos 3\Omega t\right) + \frac{Q}{32\Omega^3}\left(3 - \frac{1}{\Omega^2}\right)\left(3\sin\Omega t - \sin 3\Omega t\right) \tag{23}$$

Consequently, the following equation is obtained:

$$y_1(t-\tau) = -\frac{Q}{32\Omega^2}\left(1 - \frac{3}{\Omega^2}\right)\left[\cos\Omega(t-\tau) - \cos 3\Omega(t-\tau)\right] + \frac{Q}{32\Omega^3}\left(3 - \frac{1}{\Omega^2}\right)\left[3\sin\Omega(t-\tau) - \sin 3\Omega(t-\tau)\right]. \tag{24}$$

Inserting Eqs.(19), (22), (23), and (24) into the second-order problem as given in Eq.(18) and removing the source of secular terms yields

$$\begin{aligned} \omega_2 = &-\frac{\mu Q}{16\Omega^2}\left(1 + \Omega^2\right) - \frac{3Q^2}{128\Omega^6}\left(\Omega^4 - 18\Omega^3 - 6\Omega^2 + 8\Omega + 1\right) + \frac{3\mu Q}{64\Omega^5}\left(3\Omega^2 - 1\right)\left(\Omega\cos\Omega\tau + \sin\Omega\tau\right) \\ &- \frac{3\eta Q}{64\Omega^4}\left(3\Omega^2 - 1\right)\cos\Omega\tau + \frac{\eta Q}{64\Omega^5}\left(4\Omega^4 - 5\Omega^2 + 3\right)\sin\Omega\tau. \end{aligned} \tag{25}$$

without secular terms, the uniform solution $y_2(t)$ is written as

$$\begin{aligned}
y_2(t) &= \frac{Q\cos\Omega t}{256\Omega^4}\left[\begin{array}{l} -\frac{\mu}{2\Omega^2}\left(\Omega^4+14\Omega^2-3\right)-\frac{Q}{4\Omega^4}\left(\Omega^4-8\Omega^3+12\Omega^2+27\Omega+2\right)-\frac{\eta}{\Omega^3}\left(3-\frac{1}{\Omega^2}\right)\sin 3\Omega\tau \\ +\frac{\eta}{2}\left(1-\frac{3}{\Omega^2}\right)\left(\Omega-\frac{1}{\Omega}\right)\sin\Omega\tau+\eta\left(1-\frac{3}{\Omega^2}\right)\left(\cos 3\Omega\tau-\cos\Omega\tau\right)\end{array}\right] \\
&+\frac{Q\sin\Omega t}{256\Omega^5}\left[\begin{array}{l} -\frac{3\mu}{2\Omega^2}\left(3\Omega^4-14\Omega^2-1\right)-\frac{Q}{4\Omega^4}\left(47\Omega^4+120\Omega^3-10\Omega^2-40\Omega-9\right)-3\eta\Omega\left(1-\frac{3}{\Omega^2}\right)\sin 3\Omega\tau \\ +3\eta\left(3-\frac{1}{\Omega^2}\right)\left(3\cos 3\Omega\tau+\cos\Omega\tau\right)-\frac{3\eta}{2}\left(3-\frac{1}{\Omega^2}\right)\left(\Omega-\frac{1}{\Omega}\right)\sin\Omega\tau\end{array}\right] \\
&-\frac{Q\cos 3\Omega t}{256\Omega^4}\left[\begin{array}{l} -\frac{\mu}{2\Omega^2}\left(\Omega^4+14\Omega^2-3\right)+\frac{3Q}{4\Omega^3}\left(3\Omega^2-8\Omega-9\right)+\frac{\eta}{2}\left(1-\frac{3}{\Omega^2}\right)\left(\Omega-\frac{1}{\Omega}\right)\sin\Omega\tau \\ -\eta\left(1-\frac{3}{\Omega^2}\right)\cos\Omega\tau\end{array}\right] \\
&-\frac{Q\sin 3\Omega t}{256\Omega^5}\left[\begin{array}{l} -\frac{\mu}{2\Omega^2}\left(3\Omega^4-14\Omega^2-1\right)-\frac{3Q}{4\Omega^4}\left(8\Omega^4+15\Omega^3-5\Omega^2-5\Omega-1\right)+\eta\left(3-\frac{1}{\Omega^2}\right)\cos\Omega\tau \\ -\frac{\eta}{2}\left(3-\frac{1}{\Omega^2}\right)\left(\Omega-\frac{1}{\Omega}\right)\sin\Omega\tau\end{array}\right] \\
&+\frac{Q^2}{1024\Omega^8}\left(\Omega^4+\Omega^3-12\Omega^2+2\right)\cos 5\Omega t-\frac{Q^2}{1024\Omega^8}\left(5\Omega^3+3\Omega^2-7\Omega-1\right)\sin 5\Omega t \\
&-\frac{\eta Q}{256\Omega^4}\left(1-\frac{3}{\Omega^2}\right)\cos 3\Omega(t-\tau)-\frac{\eta Q}{256\Omega^5}\left(3-\frac{1}{\Omega^2}\right)\sin 3\Omega(t-\tau).
\end{aligned} \tag{26}$$

Therefore, the complete approximate solution is formulated by substituting Eqs. (19), (23) and (26) into Eq. (6) along with setting $\rho\to 1$ to obtain the following equation:

$$\begin{aligned}
y(t) &= \cos\Omega t-\frac{1}{\Omega}\sin\Omega t \\
&+\frac{Q\cos\Omega t}{256\Omega^4}\left[\begin{array}{l} -8\Omega^2\left(1-\frac{3}{\Omega^2}\right)-\frac{Q}{4\Omega^4}\left(\Omega^4-8\Omega^3+12\Omega^2+27\Omega+2\right)-\frac{\mu}{2\Omega^2}\left(\Omega^4+14\Omega^2-3\right) \\ +\eta\left(1-\frac{3}{\Omega^2}\right)\left(\cos 3\Omega\tau-\cos\Omega\tau\right)+\frac{\eta}{2}\left(1-\frac{3}{\Omega^2}\right)\left(\Omega-\frac{1}{\Omega}\right)\sin\Omega\tau-\frac{\eta}{\Omega^3}\left(3-\frac{1}{\Omega^2}\right)\sin 3\Omega\tau\end{array}\right] \\
&+\frac{Q\sin\Omega t}{256\Omega^5}\left[\begin{array}{l} 24\Omega^2\left(3-\frac{1}{\Omega^2}\right)-\frac{Q}{4\Omega^4}\left(47\Omega^4+120\Omega^3-10\Omega^2-40\Omega-9\right)-\frac{3\mu}{2\Omega^2}\left(3\Omega^4-14\Omega^2-1\right) \\ +3\eta\left(3-\frac{1}{\Omega^2}\right)\left(3\cos 3\Omega\tau+\cos\Omega\tau\right)-\frac{3\eta}{2}\left(3-\frac{1}{\Omega^2}\right)\left(\Omega-\frac{1}{\Omega}\right)\sin\Omega\tau-3\eta\Omega\left(1-\frac{3}{\Omega^2}\right)\sin 3\Omega\tau\end{array}\right] \\
&-\frac{Q\cos 3\Omega t}{256\Omega^4}\left[\begin{array}{l} -8\Omega^2\left(1-\frac{3}{\Omega^2}\right)-\frac{\mu}{2\Omega^2}\left(\Omega^4+14\Omega^2-3\right)+\frac{3Q}{4\Omega^3}\left(3\Omega^2-8\Omega-9\right)-\eta\left(1-\frac{3}{\Omega^2}\right)\cos\Omega\tau \\ +\frac{\eta}{2}\left(1-\frac{3}{\Omega^2}\right)\left(\Omega-\frac{1}{\Omega}\right)\sin\Omega\tau\end{array}\right] \\
&-\frac{Q\sin 3\Omega t}{256\Omega^5}\left[\begin{array}{l} 8\Omega^2\left(3-\frac{1}{\Omega^2}\right)-\frac{3Q}{4\Omega^4}\left(8\Omega^4+15\Omega^3-5\Omega^2-5\Omega-1\right)-\frac{\mu}{2\Omega^2}\left(3\Omega^4-14\Omega^2-1\right) \\ -\frac{\eta}{2}\left(3-\frac{1}{\Omega^2}\right)\left(\Omega-\frac{1}{\Omega}\right)\sin\Omega\tau+\eta\left(3-\frac{1}{\Omega^2}\right)\cos\Omega\tau\end{array}\right] \\
&+\frac{Q^2}{1024\Omega^8}\left(\Omega^4+\Omega^3-12\Omega^2+2\right)\cos 5\Omega t-\frac{Q^2}{1024\Omega^8}\left(5\Omega^3+3\Omega^2-7\Omega-1\right)\sin 5\Omega t \\
&-\frac{\eta Q}{256\Omega^4}\left(1-\frac{3}{\Omega^2}\right)\cos 3\Omega(t-\tau)-\frac{\eta Q}{256\Omega^5}\left(3-\frac{1}{\Omega^2}\right)\sin 3\Omega(t-\tau).
\end{aligned} \tag{27}$$

The above-mentioned approximate solution is formulated as a function of all parameters of the problem. It contains periodic functions in the independent variable t as well as the time-delayed parameter τ, assuming that the nonlinear frequency Ω has real values. The second-order approximation of the nonlinear frequency Ω can be formulated by substituting Eqs. (22) and (25) into Eq. (5) along with setting $\rho \to 1$ to obtain the following equation:

$$\begin{aligned}\Omega^2 &= \omega^2 + \tfrac{1}{2}\left(1-\Omega^2\right)\mu + \frac{3Q}{4}\left(1+\frac{1}{\Omega^2}\right) + \tfrac{1}{2}\eta\left(\Omega - \frac{1}{\Omega}\right)\sin\Omega\tau - \eta\cos\Omega\tau - \frac{\mu Q}{16\Omega^2}\left(1+\Omega^2\right) \\ &- \frac{3Q^2}{128\Omega^6}\left(\Omega^4 - 18\Omega^3 - 6\Omega^2 + 8\Omega + 1\right) + \frac{3\mu Q}{64\Omega^5}\left(3\Omega^2 - 1\right)\left(\Omega\cos\Omega\tau + \sin\Omega\tau\right) \\ &- \frac{3\eta Q}{64\Omega^4}\left(3\Omega^2 - 1\right)\cos\Omega\tau + \frac{\eta Q}{64\Omega^5}\left(4\Omega^4 - 5\Omega^2 + 3\right)\sin\Omega\tau.\end{aligned} \tag{28}$$

This relation shows that the approximate nonlinear frequency Ω is a function in each of the linear frequency ω, damping parameter μ, coefficient of the delayed term η, nonlinear coefficient Q, and the time-delayed parameter τ. The nonlinear frequency appears as a periodic function in the time-delayed parameter. This is the nonlinear characteristic equation which has a transcendental form in the frequency Ω. Its Eigen values are impossible to obtain analytically, therefore, the stability criteria are very difficult to catch from this complicated equation.

3. Numerical Illustration of Complete Solution by the Frequency Analysis

The nonlinear frequency (Eq. (28)) is plotted in three graphs as given in Figs. (1), (2), and (3) to show the distribution of the linear frequency ω^2 versus the variation of the nonlinear frequency Ω in the absence of the delayed part, while other parameters are kept fixed. As can be seen in Fig. (1), the relation between linear frequency and nonlinear frequency such as the exponential behavior is shown. When the delayed coefficient is included ($\eta = 7$ and $\tau = 10$), the exponential profile has a period form as shown in Fig (2). In Fig (3), the frequency ω^2 is plotted versus the delayed parameter τ at fixed Ω. This graph shows the periodic form of the nonlinear frequency with respect to the time delay.

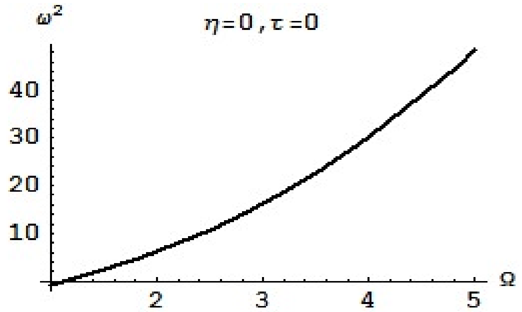

Fig. 1. The distribution of the linear frequency versus the variation of the nonlinear frequency.

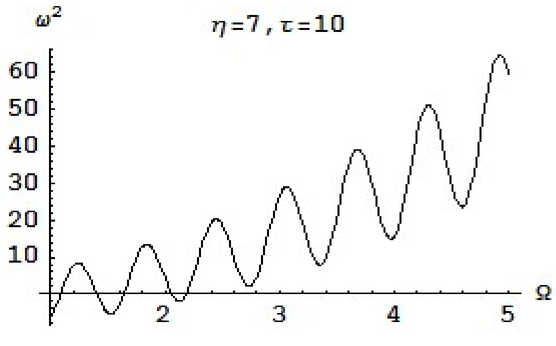

Fig. 2. The relation given in Fig. 1. when the delayed term has non-zero values.

The complete periodic solution, as given in Eq. (26), is illustrated graphically. Several numerical calculations are presented along with Figs. (4) to (9). In these figures, the function $y(t)$ is plotted versus the variation of the independent variable t. The vertical axis represents the distribution of the function $y(t)$, and the horizontal axis refers to the variations of the time t. In these figures, three different values of a specific parameter are considered, while the other parameters are kept fixed. The $y-curve$, as shown in Fig. (4), is plotted for a system having the particulars: $\omega^2 = 0, \omega^2 = 5, \omega^2 = 10, \Omega = 3$ and $\mu = 1$, $Q = 5, \eta = 2, \tau = 10$. These three cases are described as follows: At $t = 0$, the three curves are started from the same point on the y-coordinate. Moreover, it is observed that the curves have a periodic behavior of the same amplitude. Finally, the three curves are corresponding to $\omega^2 = 0$, $\omega^2 = 5$, and $\omega^2 = 10$. The solid curve indicates the case at which $\omega^2 = 0$, the dashed curve refers to the case of $\omega^2 = 5$ and the dotted case stands for the case when $\omega^2 = 10$. This mechanism shows the increase of the linear frequency ω^2 which plays a stabilizing role.

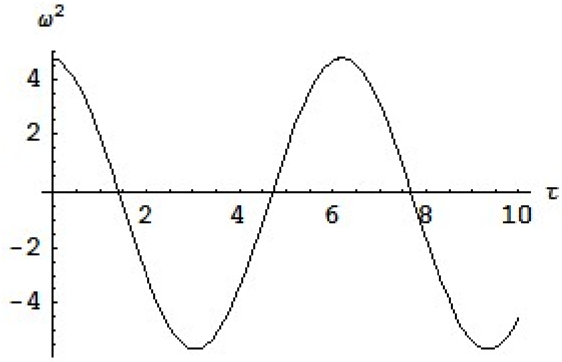

Fig. 3. The distribution of the frequency against the time-delay.

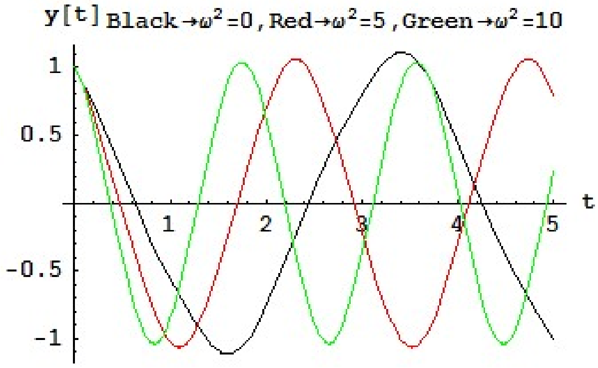

Fig. 4. The distribution for the y-curve, as a function in ω^2, against the variation in the time t.

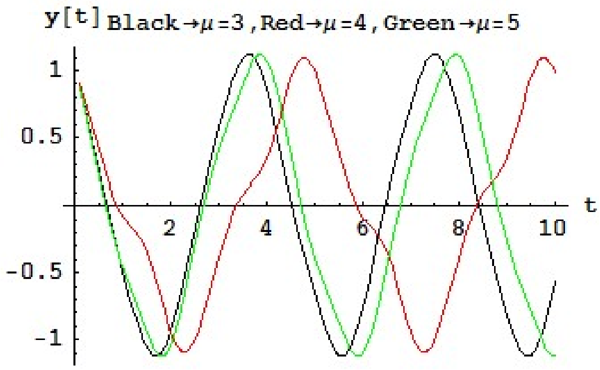

Fig. 5. The distribution for the y-curve, as a function in μ, against the variation in the time *t*.

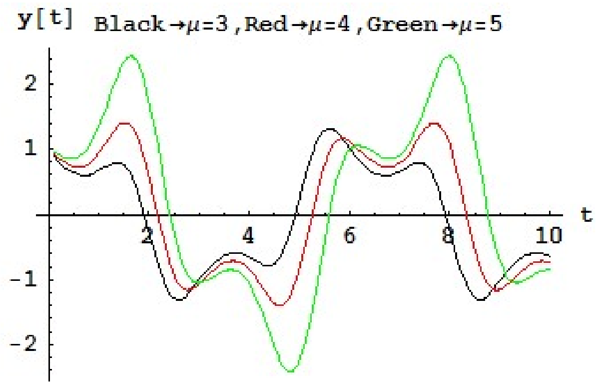

Fig .6. This graph is the same as Fig. (5) except for large values in the time-delay.

As can be seen, Fig. (5) illustrates the influence of the variations of the damping parameter μ on the $y(t)-curve$ for a system having the fixed parameters $\omega^2 = 1, Q = 3, \eta = 2, \tau = 10$ and $\Omega = 3$. In these cases, the damped parameters are given as $(\mu = 3, 4, 5)$. It is observed that the length of segment between the started point and the first most upper point increased as μ is changed from $\mu = 3$ to $\mu = 4$ and decreased when it is changed from $\mu = 4$ to $\mu = 5$. This means that there is a destabilizing effect in the first case and a stabilizing influence in the other case. The increase in the time-delayed parameter from $\tau = 10$ to $\tau = 11$, for the same system given in Fig. (5), leads to more changes in the profile of the graph as shown in Fig. (6). The most-upper point rises in the direction of increasing y-axis for the small time t. For increasing the time t, a rise in the upper point in the opposite direction is observed. As the time *t* is increased, the first role is changed.

The examination of the nonlinear coefficient Q is shown in Fig. (7). It is shown that there are two roles depicted in the stability picture. Small destabilizing influence for increasing in the coefficient η is observed (Fig. (8)). This destabilizing influence is observed as t increases. The examination of the time-delay τ is the aim of the graph given in Fig. (9) in which the dual role is observed.

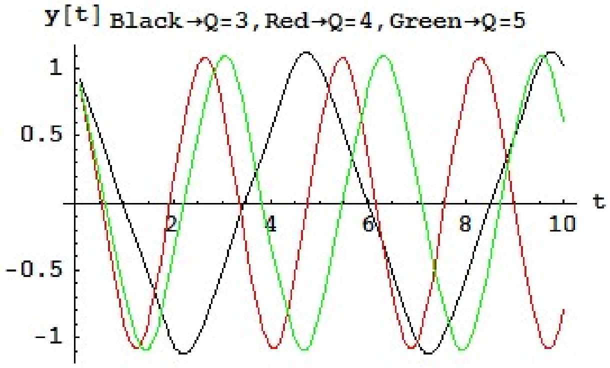

Fig. 7. The distribution for the y-curve, as a function in Q, against the variation in the time *t*.

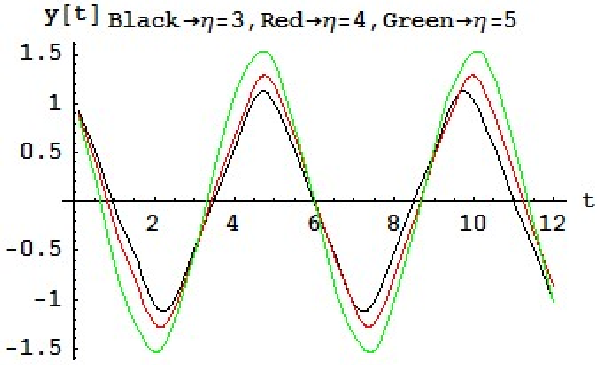

Fig. 8. The distribution for the y-curve, as a function in η, versus the variation in the time *t*.

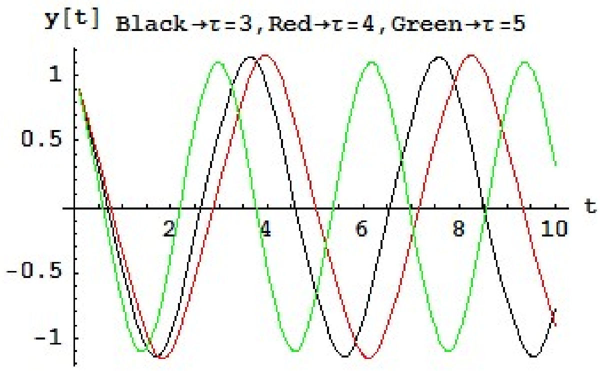

Fig. 9. The distribution for the y-curve, as a function in τ, versus the variation in the time *t*.

4. Multiple-Scales Homotopy Perturbation Approach for Delayed Duffing Oscillator

The multiple scales method is a well-known method in the perturbation theory. It is effective for weakly nonlinear oscillators [39 & 40]. However, the combination of the homotopy perturbation method with the multiple scales method yields an unexpected result and allows studying the stability behavior for strongly nonlinear oscillators [26]. Two parts for the nonlinear Eq. (1) are described as:

$$L(y)=\frac{d^2y}{dt^2}+\omega^2 y,\quad N(y)=\mu\frac{dy}{dt}+Qy^3-\eta y\left(t-\tau\right). \tag{29}$$

The homotop-multiple-scales statement is constructed in the following form:

$$H\left(y,\rho\right)=\left(\frac{d^2}{dt^2}+\omega^2\right)y\left(t,\rho\right)+\rho\left[\mu\frac{dy\left(t,\rho\right)}{dt}+Qy^3\left(t,\rho\right)-\eta y\left(t-\tau,\rho\right)\right]=0. \tag{30}$$

Therefore, $\lim_{\rho\to1}H\left(y,\rho\right)=0$ gives the original relation as given in Eq. (1). Consequently, the following relation is obtained:

$$\lim_{\rho\to0}H\left(y,\rho\right)=\left(\frac{d^2}{dt^2}+\omega^2\right)y\left(t,\rho\right)=0. \tag{31}$$

According to the expansion as given by Eq. (11) and considering three-time scales $T_0=t, T_1=\rho t, T_2=\rho^2 t$, the function $y\left(t-\tau,\rho\right)$ becomes

$$y\left(t-\tau,\rho\right)=Y_0\left(T_0-\tau,T_1-\rho\tau,T_2-\rho^2\tau\right)+\rho Y_1\left(T_0-\tau,T_1-\rho\tau,T_2-\rho^2\tau\right)+... \tag{32}$$

Using Taylor expansion, the following relation is obtained:

$$\begin{aligned}Y_n\left(T_0-\tau,T_1-\rho\tau,T_2-\rho^2\tau\right)&=\left[1-\tau\left(\rho D_1+\rho^2 D_2+...\right)+\tfrac{1}{2}\tau^2\left(\rho D_1+\rho^2 D_2+...\right)^2\right]Y_n(T_0-\tau,T_1,T_2)\\&=\left[1-\rho\tau D_1+\rho^2\left(\tfrac{1}{2}\tau^2 D_1^2-\tau D_2\right)+...\right]Y_n(T_0-\tau,T_1,T_2),\end{aligned} \tag{33}$$

where $D_n\equiv d/dT_n$. Employing Eqs. (8-10) along with the homotopy Eq. (30), using Eqs. (32) and (33), and then rearranging the result in a power series of ρ yield

$$H(y,\rho)=H_0+\rho H_1+\rho^2 H_2+\rho^3 H_3+...=0, \tag{34}$$

where

$$H_0=\lim_{\rho\to0}H(y,\rho),\quad \text{and}\quad H_n=\frac{1}{n!}\lim_{\rho\to0}\frac{\partial^n H(y,\rho)}{\partial\rho^n}. \tag{35}$$

Accordingly, the following equations are obtained:

$$H_0=0,\ H_1=0,\ H_2=0,..., \tag{36}$$

$$H_0(y_0)=D_0^2 y_0+\omega^2 y_0=0, \tag{37}$$

$$H_1(y_0,y_1)=D_0^2 y_1+\omega^2 y_1+2D_0D_1y_0+\mu D_0 y_0+Qy_0^3-\eta y_0\left(T_0-\tau,T_1,T_2\right)=0, \tag{38}$$

$$\begin{aligned}H_2(y_0,y_1,y_2)=D_0^2 y_2+\omega^2 y_2+2D_0D_1y_1+\left(D_1^2+2D_0D_2\right)y_0+\mu D_0 y_1+\mu D_1 y_0+3Qy_1y_0^2\\-\eta y_1\left(T_0-\tau,T_1,T_2\right)+\eta\tau D_1 y_0\left(T_0-\tau,T_1,T_2\right)=0,\end{aligned} \tag{39}$$

These equations are inhomogeneous linear equations. The presence of the inhomogeneity produces secular terms. Solving theses equations and excluding the secular terms in each stage, uniform solutions $y_0, y_1, y_2,...$ are obtained in the following forms:

$$y_0(T_0,T_1,T_2)=A(T_1,T_2)e^{i\omega T_0}+\bar{A}(T_1,T_2)e^{-i\omega T_0}, \tag{40}$$

$$y_0(T_0-\tau,T_1,T_2)=A(T_1,T_2)e^{i\omega(T_0-\tau)}+\bar{A}(T_1,T_2)e^{-i\omega(T_0-\tau)}, \tag{41}$$

$$y_1(T_0,T_1,T_2)=\frac{Q}{8\omega^2}\left(A^3e^{3i\omega T_0}+\bar{A}^3e^{-3i\omega T_0}\right), \tag{42}$$

$$y_1(T_0-\tau,T_1,T_2)=\frac{Q}{8\omega^2}\left(A^3e^{3i\omega(T_0-\tau)}+\bar{A}^3e^{-3i\omega(T_0-\tau)}\right), \tag{43}$$

$$\begin{aligned}y_2(T_0,T_1,T_2)=\frac{Q^2}{64\omega^4}\left(A^5e^{5i\omega T_0}+\bar{A}^5e^{-5i\omega T_0}\right)-\frac{3Q^2}{64\omega^4}A\bar{A}\left(A^3e^{3i\omega T_0}+\bar{A}^3e^{-3i\omega T_0}\right)\\+\frac{Q}{64\omega^4}\left[\eta\left(3e^{-i\omega\tau}-e^{-3i\omega\tau}\right)A^3e^{3i\omega T_0}+\eta\left(3e^{i\omega\tau}-e^{3i\omega\tau}\right)\bar{A}^3e^{-3i\omega T_0}\right].\end{aligned} \tag{44}$$

The above-mentioned analysis yields the following two solvability conditions:

$$D_1 A + \tfrac{1}{2}\mu A + i\,\frac{\eta}{2\omega} e^{-i\omega\tau} A - \frac{3iQ}{2\omega} A^2 \bar{A} = 0, \tag{45}$$

$$2i\,\omega D_2 + D_1^2 A + \mu D_1 A + \eta\tau D_1 A e^{-i\omega\tau} + \frac{3Q^2}{8\omega^2} A^3 \bar{A}^2 = 0. \tag{46}$$

The amplitude Eq. (45) results from the first-order perturbation. Meanwhile, Eq. (46) is obtained from the second-order perturbation. The later equation contains derivatives with respect to T_1 and T_2. Removing the derivatives with respect to T_1 with the help of Eq. (45) leads to

$$\begin{aligned} &D_2 A + \frac{i}{4\omega}\mu\left[\tfrac{1}{2}\mu + \eta\tau\left(\cos\omega\tau - i\sin\omega\tau\right)\right]A + \frac{i\eta^2}{8\omega^3}\left[\left(\cos 2\omega\tau + 2\omega\tau\sin 2\omega\tau\right) + i\left(2\omega\tau\cos 2\omega\tau - \sin 2\omega\tau\right)\right]A \\ &-\frac{3Q}{4\omega^2}\left[-\mu + \frac{\eta}{\omega}\left(\omega\tau\cos\omega\tau - 2\sin\omega\tau\right) - i\,\frac{\eta}{\omega}\left(\omega\tau\sin\omega\tau + \cos\omega\tau\right)\right]A^2\bar{A} + i\,\frac{15Q^2}{16\omega^3}A^3\bar{A}^2 = 0. \end{aligned} \tag{47}$$

The stability behavior is produced by solving Eqs. (45) and (47). For this purpose, integrate Eq. (45) with respect to T_1, and then integrate Eq. (47) with respect to T_2. Consequently, the integration of the amplitude equations is obtained in the original variable t and Eqs. (45) and (47) are combined. This combination is achieved by multiply Eqs. (45) and (47) with ρ and ρ^2, respectively. In this stage, the amplitude functions and the expansion of the derivative $\left(\rho D_1 + \rho^2 D_2\right)A\left(T_1, T_2\right)$ becomes $d/dt[A(t)]$. Finally, the following equation that governs the amplitude equation is obtained:

$$\begin{aligned} &\frac{d}{dt}A + \frac{1}{8\omega^3}\left[4\mu\omega^2\left(\omega + \tau\sin\omega\tau\right) + 4\omega^2\eta\sin\omega\tau + \eta^2\left(\sin 2\omega\tau - 2\omega\tau\cos 2\omega\tau\right)\right]A + \\ &+i\,\frac{1}{8\omega^3}\left[\mu\omega^2\left(\mu + 2\eta\tau\cos\omega\tau\right) + 4\omega^2\eta\cos\omega\tau + \eta^2\left(\cos 2\omega\tau + 2\omega\tau\sin 2\omega\tau\right)\right]A \\ &+\frac{3Q}{4\omega^2}\left\{\mu - \frac{\eta}{\omega}\left(\omega\tau\cos\omega\tau - 2\sin\omega\tau\right) - 2i\,\omega + i\,\frac{\eta}{\omega}\left(\omega\tau\sin\omega\tau + \cos\omega\tau\right)\right\}A^2\bar{A} + i\,\frac{15Q^2}{16\omega^3}A^3\bar{A}^2 = 0. \end{aligned} \tag{48}$$

This equation (Eq. (48)) is a nonlinear first-order differential equation having complex coefficients and is used to discuss the stability criterion of the problem. This equation is satisfied by using the following transformation:

$$A(t) = B(t)e^{-i\varpi t}, \tag{49}$$

where $B(t)$ is a time-dependent function, and ϖ is given by:

$$\varpi = \frac{1}{8\omega^3}\left[\mu^2\omega^2 + \eta^2\left(\cos 2\omega\tau + 2\omega\tau\sin 2\omega\tau\right) + 2\eta\omega^2\left(2 + \mu\tau\right)\cos\omega\tau\right], \tag{50}$$

$$\begin{aligned} &\frac{d}{dt}B + \varpi B + \frac{3Q}{4\omega^3}\left[\mu\omega - \eta\left(\omega\tau\cos\omega\tau - 2\sin\omega\tau\right) - 2i\,\omega^2 + i\,\eta\left(\omega\tau\sin\omega\tau + \cos\omega\tau\right)\right]B^2\bar{B} \\ &+i\,\frac{15Q^2}{16\omega^3}B^3\bar{B}^2 = 0. \end{aligned} \tag{51}$$

To obtain the solution of Eq. (51), it is convenient to use the following polar form:

$$B(t) = \tfrac{1}{2}\alpha(t)e^{i\beta(t)}. \tag{52}$$

The substitution of Eqs. (52) into (51) yields the following real and imaginary parts:

$$\frac{d}{dt}\alpha + \frac{1}{4}\sigma\alpha + \frac{3Q}{4\omega^3}\left[\mu\omega - \eta\left(\omega\tau\cos\omega\tau - 2\sin\omega\tau\right)\right]\alpha^3 = 0, \tag{53}$$

$$\frac{d}{dt}\beta + \frac{3Q}{4\omega^3}\left[-2\omega^2 + \eta\left(\omega\tau\sin\omega\tau + \cos\omega\tau\right)\right]\alpha^2 + \frac{15Q^2}{16\omega^3}\alpha^4 = 0, \tag{54}$$

where σ is given by

$$\sigma = \frac{1}{2\omega^3}\left[4\mu\omega^2\left(\omega + \tau\sin\omega\tau\right) + 4\omega^2\eta\sin\omega\tau + \eta^2\left(\sin 2\omega\tau - 2\omega\tau\cos 2\omega\tau\right)\right]. \tag{55}$$

where Eq. (53) is a nonlinear first-order differential equation with real coefficients. It has a steady-state solution α_0, such that

$$\alpha_0^2 = \frac{\left[4\mu\omega^2\left(\omega+\tau\sin\omega\tau\right)+4\omega^2\eta\sin\omega\tau+\eta^2\left(\sin 2\omega\tau-2\omega\tau\cos 2\omega\tau\right)\right]}{6Q\left[-\mu\omega+\eta\left(\omega\tau\cos\omega\tau-2\sin\omega\tau\right)\right]}, \tag{56}$$

where $\eta\omega\tau\cos\omega\tau \neq \mu\omega+2\eta\sin\omega\tau$. If the amplitude function $\alpha(t)$ is perturbed around the steady-state response, it yields

$$\alpha(t)=\alpha_0+\alpha_1(t), \tag{57}$$

where the function $\alpha_1(t)$ represents a small deviation from the steady-state response. Substituting Eq. (57) into (53), then the linearization of $\alpha_1(t)$ yields

$$\frac{d}{dt}\alpha_1-\frac{3Q}{\omega^3}\left[\mu\omega-\eta\left(\omega\tau\cos\omega\tau-2\sin\omega\tau\right)\right]\alpha_0^2\alpha_1=0. \tag{58}$$

This equation (Eq. (58)) is satisfied by

$$\alpha_1(t)=ae^{-\sigma t}, \tag{59}$$

where $a \ll 1$, is a real constant. Substituting Eq. (57) into Eq. (54) and linearizing α_1 leads to

$$\frac{d}{dt}\beta+\frac{3Q}{4\omega^2}\left[-2\omega+\frac{\eta}{\omega}\left(\omega\tau\sin\omega\tau+\cos\omega\tau\right)\right]\left(\alpha_0^2+2\alpha_0 ae^{-\sigma t}\right)+\frac{15Q^2}{16\omega^3}\left(\alpha_0^4+4\alpha_0^3 ae^{-\sigma t}\right)=0. \tag{60}$$

Integrating both sides of Eq. (60) with respect to t yields

$$\begin{aligned}\beta(t)=&-\frac{3Q}{4\omega^2}\alpha_0\left[\frac{5Q}{4\omega}\alpha_0^2-2\omega+\frac{\eta}{\omega}\left(\omega\tau\sin\omega\tau+\cos\omega\tau\right)\right]\left(\alpha_0 t+\frac{2\omega^3}{3Q\left[\mu\omega-\eta\left(\omega\tau\cos\omega\tau-2\sin\omega\tau\right)\right]\alpha_0^2}ae^{-\sigma t}\right)\\&-\frac{5Q\alpha_0}{8\left[\mu\omega-\eta\left(\omega\tau\cos\omega\tau-2\sin\omega\tau\right)\right]}ae^{-\sigma t}-b.\end{aligned} \tag{61}$$

where b is an arbitrary integration constant. Substituting Eqs. (57) and (61) into Eq. (52) and then into Eq. (49) yields

$$A(t)=\tfrac{1}{2}\left(\alpha_0+ae^{\sigma t}\right)e^{-i\varphi(t)}, \tag{62}$$

where the function $\varphi(t)$ is given by

$$\begin{aligned}\varphi(t)=&\varpi t+\frac{3Q\alpha_0^2}{16\omega^3}\left[5Q\alpha_0^2-8\omega^2+4\eta\left(\omega\tau\sin\omega\tau+\cos\omega\tau\right)+\right]t\\&+\frac{\left[5Q\alpha_0^2-4\omega^2+2\eta\left(\omega\tau\sin\omega\tau+\cos\omega\tau\right)\right]}{4\left[\mu\omega-\eta\left(\omega\tau\cos\omega\tau-2\sin\omega\tau\right)\right]\alpha_0}ae^{-\sigma t}+b.\end{aligned} \tag{63}$$

The complete primary solution $y_0(t)$ is formulated by inserting Eq. (62) into Eq. (40) and after setting $\rho\to 1$, the following relation is obtained:

$$y_0(t)=\left(\alpha_0+ae^{-\sigma t}\right)\cos\left(\omega t-\varphi(t)\right). \tag{64}$$

where the arbitrary constants a and b are determined by applying the initial conditions $y_0(0)=1$ and $\dot{y}_0(0)=-1$. These conditions lead to

$$\cos\left(\varphi(0)\right)=\frac{1}{\left(\alpha_0+a\right)} \quad \text{and} \quad \sin\left(\varphi(0)\right)=\frac{1}{\left(\alpha_0+a\right)\left(\omega+\dot{\varphi}(0)\right)}\left[\frac{\dot{\alpha}_1(0)}{\left(\alpha_0+a\right)}+1\right]. \tag{65}$$

where $\alpha_1(0)=a$, $\dot{\alpha}_1(0)=-a\,\sigma$, $\varphi(0)=m_1 a+b$, and $\dot{\varphi}(0)=m_2 a+m_3$. Squaring the first equation in (65) and adding to the square of the second equation yields the following relation, which determines the arbitrary constant a:

$$\left(a+\alpha_0-a\sigma\right)^2=\left(\alpha_0+a\right)^2\left[\left(\alpha_0+a\right)^2-1\right]\left(\omega+\dot{\varphi}(0)\right)^2. \tag{66}$$

Since $a \ll 1$, the linearization of Eq. (66) yields

$$a=\frac{\alpha_0^2\left(\alpha_0^2-1\right)\left(\omega+m_3\right)^2-\alpha_0^2}{2\left[\alpha_0\left(1-\sigma\right)-\left(\omega+m_3\right)\left(\alpha_0^4-\alpha_0^2+1\right)m_2-\alpha_0\left(2\alpha_0^2-1\right)\left(\omega+m_3\right)^2\right]}. \tag{67}$$

The arbitrary constant b is determine from Eq. (59), so that it is given by

$$\tan b=\frac{\left[\left(1-\sigma\right)a+\alpha_0\right]-\left(\alpha_0+a\right)\left(\omega+m_3+m_2a\right)\tan am_1}{\left(\omega+m_3+m_2a\right)+\left[\left(1-\sigma\right)a+\alpha_0\right]\tan am_1} \tag{68-a}$$

where $m_j, j=1,2,3$ are given by

$$\begin{aligned} m_1&=\frac{5Q\alpha_0^2-4\omega^2+2\eta\left(\omega\tau\sin\omega\tau+\cos\omega\tau\right)}{4\left[\mu\omega-\eta\left(\omega\tau\cos\omega\tau-2\sin\omega\tau\right)\right]\alpha_0},\\ m_2&=-\frac{3Q\alpha_0}{4\omega^3}\left[5Q\alpha_0^2-4\omega^2+2\eta(\cos\omega\tau+\omega\tau\sin\omega\tau)\right],\ \textit{and}\\ m_3&=\varpi+\frac{3Q\alpha_0^2}{16\omega^3}\left[5Q\alpha_0^2-8\omega^2+4\eta(\cos\omega\tau+\omega\tau\sin\omega\tau)\right], \end{aligned} \tag{68-b}$$

The investigation of the above-mentioned solution of the amplitude Eq. (48), reveals that the stability depends on the sign of the exponential σ. Therefore, the stability occurs when $\sigma<0,$ which leads to the following condition:

$$4\mu\omega^3+4\omega^2\left(\mu\tau+\eta\right)\sin\omega\tau+\eta^2\left(\sin2\omega\tau-2\omega\tau\cos2\omega\tau\right)>0. \tag{69}$$

This condition is satisfied at very small value of the parameter τ. Therefore, small values of $\left(2\omega\tau\right)$ implies that the last part of condition (69), $\left(\sin2\omega\tau-2\omega\tau\cos2\omega\tau\geq0\right)$, has no implication. Large values of the parameter τ lead the condition (69) to be false. Therefore, the above-mentioned condition shows that the amplitude of the delayed term η plays a stabilizing role the same as the coefficient of the damping term μ at small τ. On the other hand, large values in the time-delay parameter plays a destabilizing role. This conclusion is verified again after employing the numerical simulations.

To obtain the complete solution, Eqs. (64), (42), and (44) are substituted into Eq. (11) by using (62) and setting $\rho\to1$. Finally, the following uniform valid solution is obtained:

$$\begin{aligned} y\left(t\right)=&\left(\alpha_0+ae^{-\sigma t}\right)\cos\left(\omega t-\varphi(t)\right)+\frac{Q}{32\omega^2}\left[1-\frac{3Q}{32\omega^2}\left(\alpha_0+ae^{-\sigma t}\right)^2\right]\left(\alpha_0+ae^{-\sigma t}\right)^3\cos\left(3\omega t-3\varphi(t)\right)\\ &+\frac{Q\eta}{256\omega^4}\left(\alpha_0+ae^{-\sigma t}\right)^3\left[3\cos\left(3\omega t-\omega\tau-3\varphi\left(t\right)\right)-\cos\left(3\omega t-3\omega\tau-3\varphi\left(t\right)\right)\right]\\ &+\frac{Q^2}{1024\omega^4}\left(\alpha_0+ae^{-\sigma t}\right)^5\cos\left(5\omega t-5\varphi(t)\right). \end{aligned} \tag{70}$$

The above-mentioned relation is the complete second-order approximate periodic solution having a damping part and affected by the time-delay parameter.

5. Numerical Estimation of Complete Solution by Multiple-Scale HPM

In the following section, numerical calculations are made to illustrate the complete solution as given by Eq. (70). These calculations are made for the examination of the influences of the parameters μ, Q, η and τ on the distribution function $y(t)$. In these graphs, the variation of time is represented on the horizontal axis, while the vertical axis represents the distribution function $y\left(t\right)$. In each graph, three cases for one parameter are collected while the other parameters are kept fixed.

In Fig (10), three different values of the parameter μ are plotted at the fixed parameters $\omega^2=1, Q=1, \eta=4,$ and $\tau=5.$ The dual role of the stability behavior is observed as shown previously in Fig. (5). The examination of the influence of the Duffing coefficient on $y(t)$ is shown in Fig. (11). In this graph, three different values of Q are considered for a system having the particulars $\omega^2=1,\ \mu=2,\eta=3$, and $\tau=5.$ This graph shows that the increase in the nonlinear coefficient has no implication in the stability plot. This conclusion was obtained theoretically in the stability analysis as presented in condition (69), while it was not observed in the previous calculations shown in Fig. (7).

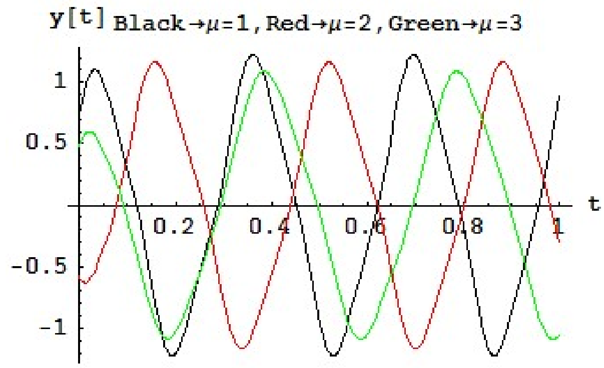

Fig. 10. The illustration for the y-curve, as a function in μ versus the variation in the time *t*.

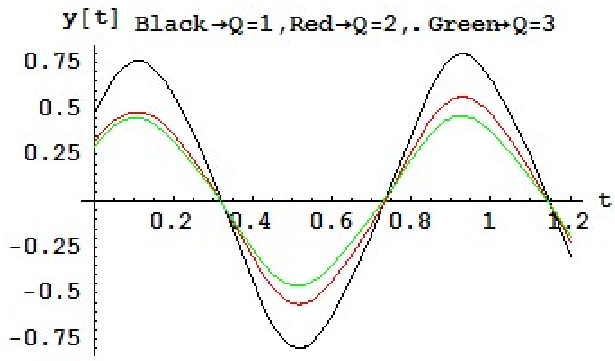

Fig. 11. The illustration for the y-curve, as a function in Q , versus the variation in the time *t*.

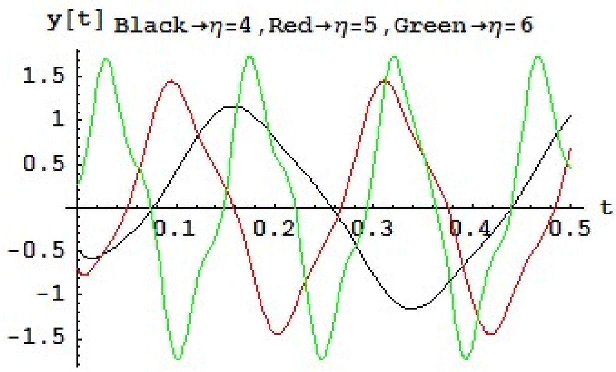

Fig. 12. The illustration for the y-curve, as a function in η, versus the variation in the time *t*.

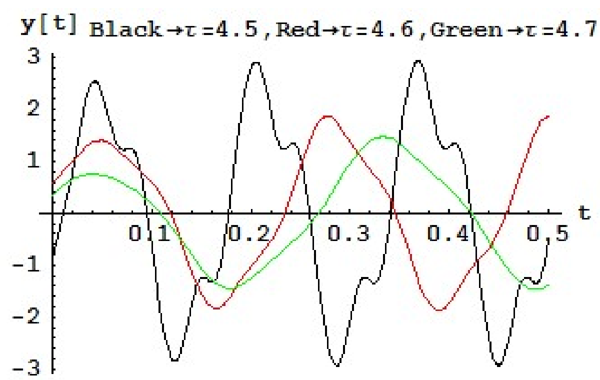

Fig. 13. The illustration for the y-curve, as a function in τ , versus the variation in the time *t*.

The above-mentioned figure (Fig (12)) indicates the influence of increasing in the parameter η on the $y(t)-curve$. The calculations are made for the system having the following parameters: $\omega^2=1, \mu=2, Q=1$ and $\tau=2$. It is shown that the increase in η has a stabilizing influence. This stabilizing effect has not been observed before in Fig. (8). The examination of the influence of the time-delay τ on the $y(t)-curve$ is shown in Fig. (13). The calculations are made for the system having the following parameters: $\omega^2 = 1, \mu = 2, Q = 1$ and $\eta = 3$. The inspection of this graph indicates that small changes in the parameter τ leads to a more shifting in the $y(t) - curve$ in the direction of increasing the time *t*, which presents a destabilizing effect on the stability configuration. On the other hand, the dual role is observed in Fig. (9) in the frequency analysis.

6. Concluding Remarks

In the present study, two analytical techniques for the homotopy perturbation method are adopted to investigate a strong delayed Duffing equation for the purpose of the comparison. The first technique is known as the frequency response analysis. In this approach, the nonlinear frequency is formulated which appears as a function of all parameters of the problem. It contains periodic terms in the time-delay from which the second-order periodic solution is derived. The corresponding numerical illustration shows that the nonlinearity has an exponential profile. This behavior has a periodic form in the time-delay τ through which the periodic solution is derived. This technique cannot be used for catching stability conditions analytically since the stability behavior is only observed in the numerical illustration. The second approach is based on a modulation of the homotopy perturbation and is used to study the stability configuration analytically. This technique is known as a multiple-scales-homotopy perturbation method in which the secularity conditions impose a nonlinear amplitude equation whose solution leads to catch the stability criterion and consequently a uniform second-order periodic solution is formulated. Then, the periodic solution is derived that contain an exponential damping part. It is found both analytically and numerically that, the time-delay parameter has a destabilizing effect while the coefficient of the delayed variable has a stabilizing one. In addition, the time-delay parameter plays a dual role in the first approach and a destabilizing influence in the second one. Moreover, in both approaches, the damping parameter has a dual influence in the stability plot while the coefficient of the delayed variable plays a destabilizing role in the first approach. In contrast, it has a stabilizing influence in the second one. On the other hand, the stabilizing influence of η is observed numerically and theoretically in the stability condition (69). The increase in the Duffing coefficient *Q* has two roles in the first approach which are disappeared in the stability condition (69). Therefore, it has no implication in the stability configuration. It is concluded that the second method is more effective than the first one and it may be extended to various linear and nonlinear problems. The multiple-scales-homotopy method is used as a powerful mathematical tool for studying the stability of nonlinear oscillator systems arising in nonlinear sciences and engineering.

References

[1] Duffing, G., Erzwungene Schwingungen bei ver¨anderlicher Eigenfrequenz und ihre Technische Beduetung, Vieweg Braunschweig, 1918.
[2] Zeeman, E. C., Duffing'equation in brain modeling, *Bulletin of the Institute of Mathematics and Its Applications*, 12(7), 1976, 207–214.
[3] Stépán, G., *Retarded Dynamical Systems: Sability and Characteristic Functions*, Longman Scientific and Technical, 1989.
[4] Nayfeh, A., Chin, C., and Pratt, J., *Applications of perturbation methods to tool chatter dynamics, in Dynamics and Chaos in Manufacturing Processes*, F. C. Moon, Ed., Wiley, 1997, 193–213,
[5] Hu, H. Y. and Wang, Z. H., *Dynamics of Controlled Mechanical Systems with Delayed Feedback*, Springer, 2002.
[6] Alhazza, K. A., Nayfeh, A. H., and Daqaq, M. F., On utilizing delayed feedback for active-multimode vibration control of cantilever beams, *Journal of Sound and Vibration*, 319(3), 2009, 735–752.
[7] Johnson, M. A., *Nonlinear differential equations with delay as models for vibrations in the machining of metals*, Ph.D. thesis, Cornell University, 1996.
[8] Hamdi, M. and Belhaq, M., Self-excited vibration control for axially fast excited beam by a time delay state feedback, *Chaos, Solitons and Fractals*, 41(2), 2009, 521-532.
[9] He, J.H., Homotopy perturbation technique, *Computer Methods in Applied Mechanics and Engineering*, 178(3-4), 1999, 257–262.
[10] He, J.H., A coupling method of a homotopy technique and a perturbation technique for non-linear problems, *International Journal of Non-Linear Mechanics*, 35(1), 2000, 37–43.
[11] He, J.H., An elementary introduction to the homotopy perturbation method, *Computers & Mathematics with Applications*, 57(3), 2009, 410–412.
[12] He, J.H., Recent development of the homotopy perturbation method, *Topological Methods in Nonlinear Analysis*, 31(2), 2008, 205–209.
[13] He, J.H., New interpretation of homotopy perturbation method, *International Journal of Modern Physics B*, 20(18), 2006, 2561–2568.
[14] He, J.H., A note on the homotopy perturbation method, *Thermal Science*, 14(2), 2010, 565-568.
[15] He, J.H., Homotopy perturbation method with two expanding parameters, *Indian Journal of Physics*, 88(2), 2014, 193-196.
[16] Rentoul, M. and Ariel, P.D., Extended homotopy perturbation method and the flow past a nonlinearly stretching sheet, *Nonlinear Science Letters A*, 2, 2011, 17–30.
[17] Abdou, M. A., Zakharov-Kuznetsov equation by the homotopy analysis method and Hirota's Bilinear method, *Nonlinear Science Letters B*, 1, 2011, 99–110.
[18] He, J.H., Some asymptotic methods for strongly nonlinear equations, *International Journal of Modern Physics B*, 20(10),

2006, 1141–1199.
[19] He, J.H., An elementary introduction to recently developed asymptotic method sand nano mechanics in textile engineering, *International Journal of Modern Physics B*, 22(21), 2008, 3487–3578.
[20] Papy, G., *Topologieals grundlage des analysis-unterrichts Vandenholck and Ruprecht, Göttingen*, Germany, 1970.
[21] He, J.H, Homotopy Perturbation Method: a new nonlinear analytical technique, *Applied Mathematics and Comp*utation, 135, 2003, 73–79.
[22] He, J.H, Homotopy Perturbation method and homotopy analysis method, *Applied Mathematics and Computation*, 156, 2004, 527–539.
[23] Liao, S.J. and Chwang, A.T., Application of homotopy analysis method in nonlinear oscillations, *Journal of Applied Mechanics*, 65, 1998, 914–922.
[24] Adamu, M.Y. and Ogenyi, P., Parameterized homotopy perturbation method, *Nonlinear Science Letters A*, 8, 2017, 240-243.
[25] El-Dib, Y.O., Homotopy Perturbation for Excited Nonlinear Equations, *Science and Engineering Applications*, 2(1), 2017, 96-108.
[26] El-Dib, Y.O., Multiple scales homotopy perturbation method for nonlinear oscillators, *Nonlinear Science Letters A*, 8(4), 2017, 352-364.
[27] Kruthika H.A., Mahindrakar, A.D. and Pasumarthy, R., Stability analysis of nonlinear time-delayed systems with application to biological models, *International Journal of Applied Mathematics and Computer Science*, 27(1), 2017, 91–103.
[28] Sheu, B., Ismail, M., E. Sanchez-Sinencio, and Wu, T.H., *Microsystems Technology for Multimedia Applications: An introduction*, New Jerstey: IEEE Press, 1995.
[29] Hamdi, M. and Belhaq, M., Control of Bistability in a Delayed Duffing Oscillator, *Advances in Acoustics and Vibratio*n, 2012, 872498, 5 pages.
[30] Rusinek, R, Weremczuk, A. and Warminski, J., Regenerative Model of Cutting Process with Nonlinear Duffing Oscillator, *Mechanics and Mechanical Engineering*, 15(4), 2011, 131–145.
[31] Liao, H., Sun, W., A new method for predicting the maximum vibration amplitude of periodic solution of non-linear system, *Nonlinear Dynamics*, 71(3), 2013, 569-582.
[32] Liao, H., Nonlinear Dynamics of Duffing Oscillator with Time Delayed Term, *Computer Modeling in Engineering and Sciences*, 103(3), 2014, 155-187.
[33] Sah, Si M. and Rand, R., Delay Terms in the Slow Flow, *Journal of Applied Nonlinear Dynamics*, 5(4), 2016, 471–484
[34] El-Dib, Y.O., Stability criterion for time-delay 3-dimension damped Mathieu equation, *Science and Engineering Applications*, 1(5), 2016, 76-88.
[35] Shakeri, F. and Dehghan, M., Solution of delay differential equations via a homotopy perturbation method, *Mathematical and Computer Modeling*, 48(3-4), 2008, 486–498.
[36] Wu, Z.-K., Solution of the ENSO delayed oscillator with homotopy analysis method, *Journal of Hydrodynamics*, 21(1), 2009, 131–135.
[37] Alomari, A. K., Noorani, M. S. and Nazar, R., Solution of delay differential equation by means of homotopy analysis method, *Acta Applicandae Mathematicae*,108(2), 2009, 395–412.
[38] Olvera, D., Elías-Zúñiga, A., López de Lacalle, L. N. and Rodríguez, C. A., Approximate Solutions of Delay Differential Equations with Constant and Variable Coefficients by the Enhanced Multistage Homotopy Perturbation Method, *Abstract and Applied Analysis*, 382475, 2014, 1-12.
[39] Nayfeh, A. H., *Perturbation Methods*, Wiley, New York, 1973.
[40] Nayfeh, A. H. and Mook, D. T., *Nonlinear Oscillations*, Wiely-Interscience, New York, 1979.
[41] Wang S. Q. and He, J. H., Nonlinear oscillator with discontinuity by parameter-expansion method, *Chaos, Solitons & Fractals*, 35, 2008, 688-691.
[42] Xu, L., Application of He's parameter-expansion method to an oscillation of a mass attached to a stretched elastic wire, Physics Letters A, 368, 2007, 259-262.
[43] Shou, D. H. and He, J. H., Application of Parameter-Expanding Method to Strongly Nonlinear Oscillators, *International Journal of Nonlinear Sciences and Numerical Simulation*, 8, 2007, 121-124.